A Mean-Field Description of Polyelectrolyte Mesogels

Sanjay Misra*

Maurice Morton Institute of Polymer Science, The University of Akron, Akron, Ohio 44325

Sasidhar Varanasi

Department of Chemical Engineering, The University of Toledo, Toledo, Ohio 43606

Received August 31, 1992; Revised Manuscript Received April 9, 1993

ABSTRACT: Microphase separation in ABA triblock copolymers creates microdomains of A blocks that are *physically* cross-linked to each other by B blocks: the so-called mesogel microstructure. The B blocks can adopt two basic conformations: they can be tethered to two A domains (bridges) or to only one A domain (loops). In this study the lamellar morphology of these mesogels is considered. The B block is considered to be a polyelectrolyte with a backbone that can be hydrophobic. Swelling of such gels in aqueous media is theoretically explored—specifically two limits are explored (i) the salt dominance limit and (ii) the no salt limit. Equilibrium swelling characteristics of these gels as well as the response to external pressure, in the swollen state, are predicted. In the high salt concentration regime a continuous transition from the collapsed to swollen state is observed for changes in the backbone solvancy. The collapse transition is unaffected, in the salt dominance limit, by the fraction of loops or bridges. The elongation in salt dominance strongly depends upon the loop fraction, but the compression is independent of the loop fractions. A strong contrast is seen in the no salt limit case where the collapse transition is discontinuous with changing excluded volume (or charge fraction) and hysteresis can be observed. The collapse transition is now affected by the loop fraction—indeed critical behavior is observed with changing loop fraction. The elongation and compression are both affected by the loop fraction in the no salt limit.

1. Introduction

The fact that long-chain polymers are rarely miscible is well-known. Phase separation in block copolymers made from immiscible polymer blocks leads to a variety of very interesting microstructures.[1–3]

A distinctive feature of phase separation in block copolymer melts is the fact that macrophase separation is suppressed due to the connectedness of the incompatible blocks. Instead microphase separation leads to the formation of microdomains, rich in one or the other component of the chain, whose dimensions are of the same order as the dimensions of the individual blocks. For sufficiently high incompatibility, usually obtained for long-chain polymers, another distinctive feature arises—the so-called tethering of the junction of the blocks.[3] In this limit the junctions of the two blocks are confined to an interface that is extremely narrow compared to the dimensions of the microdomains—the so-called strong segregation regime. The tethered picture visualizes segregated block copolymer melts as microdomains containing only one component, the block junctions lying at the interface between the domains. These domains may acquire various geometrics (lamellar, cylindrical, spherical, etc.) depending upon relative block lengths as well as the degree of incompatibility.[3]

The situation of current interest involves symmetric triblock copolymers of the kind A–B–A. Again, given sufficient incompatibility, one obtains a segregated morphology with microdomains containing only A chains or only B chains (Figure 1). While microphase-separated triblocks form microstructures similar in many aspects to those formed by diblocks, the presence of *physical cross-linking* in the former is a novel feature. Physical cross-linking in triblock copolymers arises from the fact that the end A blocks have the option of remaining in the same microdomain and forming a "loop" or getting entangled in two different domains and forming a "bridge". The bridges act as *cross-links*, giving the structure mechanical properties strikingly different from a similar microstructure formed by diblock copolymers—i.e., triblock copolymer melts are elastic not fluid.

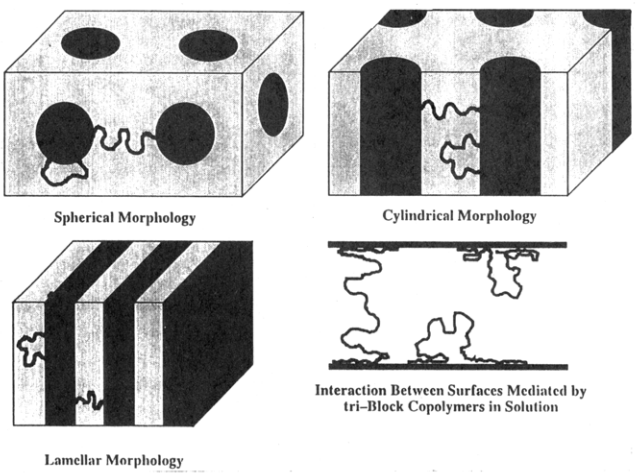

Figure 1. Typical morphologies formed by the microphase separation of ABA triblock copolymers in melts. Also illustrated is the interaction between two surfaces mediated by triblock copolymers. The two conformations, loops and bridges, are depicted as well.

The situation of particular interest, proposed recently by Halperin and Zhulina, arises upon the addition of a selective solvent for the center B blocks to the microstructure. In this case one gets a swollen network of B chains tethered to the A microdomains, the A microdomains playing the role of cross-links.[4,5] The swollen mesogel is like a mixed brush composed of (B) chains tethered at *both* ends. The A domains retain their stability as long as the solvent does not penetrate them (high solvent incompatibility), they are below their glass transition temperature (frozen), or they are selectively cross-linked. The swollen structure is reminiscent of the commonly encountered *chemically* cross-linked gels except that here the gel results from the mesophases of the microphase-separated triblock copolymers. The name *mesogel* was

* Author to whom correspondence should be addressed.

0024-9297/93/2226-4184$04.00/0

thus coined by Halperin and Zhulina to describe the swollen structure. In the context of neutral, i.e., uncharged, polymer chains Halperin and Zhulina have proposed both scaling[4] and rigorous self-consistent-field (SCF)[5] approaches recently. They have looked at both equilibrium swelling characteristics and the response of the gel to elongational and shear stresses.

In the context of uncharged polymers the studies on the stretching of brushes in good solvents by Rabin and Alexander[6] and in poor solvents by Halperin and Zhulina[7] are also relevant. These correspond to mesogels with no loops (all bridges) and show phase transitions in the presence of applied force.

The relevance of studying mesogels lies in the numerous application of block copolymers in the engineering of materials, in adhesives, or as compatibilizers.[8,9] Indeed another situation closely resembling mesogels is the interaction between two surfaces mediated by triblock copolymers.[10] Thus a study of the swelling and compression of mesogels is directly relevant to the study of interactions between two surfaces carrying adsorbed ABA triblock copolymers (with A being the adsorbing block; see Figure 1). Finally, as pointed out by Halperin and Zhulina,[5] mesogels could provide *macroscopic* systems for direct studies on brush conformations, in contrast to the microscopic studies involving force measurements on single layers of brushes (see, for example, ref 10).

Addition of electrostatic charges to the polymer can lead to an interesting range of phenomena associated with swollen mesogels. In this study therefore the focus is upon the lamellar morphology of phase-separated ABA triblock copolymers, where the B block is a *polyelectrolyte*. A simple mean-field model is developed here, taking into account explicitly the electrostatic and excluded-volume interactions, in order to predict the swelling and collapse characteristics of the polyelectrolyte mesogel in aqueous media. The variables of interest are the fraction of loops and the relative strengths of electrostatic and excluded-volume forces. The A blocks, assumed to be hydrophobic, form domains that remain unswollen upon addition of an aqueous solvent. The center B block is assumed to be a polyelectrolyte with a hydrophobic backbone in general (i.e., having an excluded-volume parameter less than zero). We also study the response of the gel to external pressure in the *swollen* state.

The rest of the paper is organized as follows. In section 2 a simple model for segment density distribution inside a swollen mesogel is presented. The advantages as well as the limitations in this approach are enumerated at the end of this section. In section 3 the mean-field free energy of the mesogel is formulated for the two ends of the spectrum: one where the added electrolyte dominates the electrostatic part of free energy and the other where the mesogel is free of any mobile electrolyte. The equilibrium dimensions of the gel and the pressure needed for altering these dimensions (in the swollen state) are related to the mean-field free energy formulation. In section 4 the salient results of this study are discussed separately for the two limiting cases of salt concentrations. In section 5 qualitative insights into the effects of the loop fraction and of the relative strengths of excluded volume and electrostatics, upon the mesogel behavior, are summarized.

2. Segment Density Distribution

The junctions of the blocks are assumed to lie at the planar interfaces separating the lamellar microdomains. The A microdomains being "frozen", the density of the junctions at the interface and the fraction of chains in loops are assumed to be constant in the swollen mesogel. In general, these quantities depend upon the block lengths and incompatibility.[5] Denoting the tethering density as σ and the fraction of these tethering points employed by the loops as f, we have the following number of loops and bridges respectively per unit area

$$n_L = \sigma f \tag{1}$$

$$n_B = \sigma(1-f) \tag{2}$$

Each B block is assumed to contain N segments of length a each. We denote the dimension of the swollen B domain as $2L$.

In our mean-field picture we assume that all loops are equally stretched to a length l. This length would be smaller than half the length of the B domain, viz., $l < L$. There are thus two types of regions inside the B domain, one next to the A–B interface where segments from both loops and bridges are present and the central region containing only the bridging segments. The bridges are assumed to be *piecewise* uniformly stretched in these two regions. We assume that a fraction q of the segments from each bridge belongs to the central region.

The segment density (volume fraction) in the region near the A–B interface, denoted as Φ_{BL} (for bridge *and* loop), is thus given as:

$$\Phi_{BL} = \frac{\sigma f}{2l}Na^3 + \frac{\sigma(1-f)}{2l}(1-q)Na^3 \tag{3}$$

The first term on the right-hand side is the contribution to the segment volume fraction from the loops, while the second term is the contribution from the bridges. The segment density in the central region, denoted Φ_B (for bridge only), is given as:

$$\Phi_B = \frac{\sigma(1-f)}{2(L-l)}qNa^3 \tag{4}$$

Introducing $\bar{\sigma} = \sigma a^2$ as the dimensionless tethering density, $\beta = 2L/Na$ as the dimensionless domain length, and $\xi = l/L$ as the dimensionless loop size, one can rewrite eqs 3 and 4 succinctly as:

$$\Phi_{BL} = \frac{\bar{\sigma}}{\beta\xi}[f + (1-f)(1-q)] \tag{5}$$

$$\Phi_B = \frac{\bar{\sigma}(1-f)q}{\beta(1-\xi)} \tag{6}$$

It must be noted that upon collapse the B domain size does not become zero. The gel collapses until the volume fraction in the B domain equals unity. Thus the minimum value of the B domain dimension β is given by

$$\beta_{min} = \bar{\sigma} \tag{7}$$

Also the fractional loop size need not equal unity, even for a collapsed gel—the central region, in general, does not vanish upon compression. (This happens only in the limit of the loop fraction, $f \to 1$.) In fact for varying loop fractions, as discussed in section 4, the loop size tends to a limiting value upon the collapse of the gel. This, as discussed in that section, leads to some very interesting qualitative behavior.

A word about the stepwise density profile inside the swollen B domain. The above situation implies that all loop midpoints lie on a plane at a distance ξ (or l) from the interface. In principle, these midpoints would be distributed throughout the bridge and loop region, with a dead zone of length $2(1-\xi)$ (or $2(L-l)$) around the center of the B domain as shown by the full self-consistent-field approach of Halperin and Zhulina.[5] We would expect the current approximation to work best for strong defor-

mation cases, while the overestimation of the loop energy would increase as we approach weak deformation.

The approximation in the current work is similar to the Alexander–de Gennes ansatz of all chain ends in a brush lying in the same plane.[11,12] While there is a nonzero probability of finding the chain ends inside the whole brush as shown by Semenov[13] and Milner, Witten, and Cates (MWC),[14] the Alexander–de Gennes ansatz correctly reproduces the essential physics of the brushes and finds scaling laws that are confirmed by the full SCF approach of MWC.

The extension of the full SCF approach to polyelectrolyte mesogels along the lines of the mesogel theory of Halperin and Zhulina[5] and Johner and Joanny's theory for bridging through telechelic polymers[15] will indeed present a more accurate picture. This approach (along the lines of Miklavic and Marcelja's[16] and Misra et al.'s[17] extension of the MWC brush theory for polyelectrolytes) is numerically more involved and will be presented in another work. The current objective is to present a numerically simple model that forms an accurate qualitative description of swollen polyelectrolyte mesogels. For this purpose the present model, like the models of Borisov et al.,[18] Pincus,[19] and Ross and Pincus[20] for polyelectrolyte brushes, is quite sufficient.

3. Mean-Field Free Energy

The free energy of the blocks in the B domain is made up of contributions from their elastic stretching, excluded-volume interactions with other chains and from electrostatic interactions between the segments.

3.1. Free Energy Density of Mixing. In general, one needs to sum the contributions from the translational entropy of the solvent and the counterions (the polymer chains are tethered) as well as their interaction energies, both electrostatic and nonelectrostatic, in order to formulate the free energy density of mixing of a mesogel. The full SCF formalism would entail the simultaneous solution to the Poisson–Boltzmann (PB) equation in order to obtain the electrostatic potential distribution. However, the fact that we have assumed a stepwise density profile and the fact that the electrostatic screening length is much smaller that the B domain size[17-20] lead to a simpler picture. Here we discuss two limiting cases of interest where the picture is free from numerical complications that accompany the solution to the PB equation. These are the high salt concentration (or salt dominance) regime and the opposite limit when the mesogel contains no added salt. In this study the focus is upon those regimes which have benefited from recent insights into the nature of polyelectrolyte solutions. The mean-field formulation presented here is valid for moderate-volume fractions. The dilute limit would be corrected along the lines of MWC's modification of the brush theory for dilute layers. This approach is equivalent to the Halperin–Zhulina scaling approach.[4] The high polymer concentration limit is easily incorporated using, for example, the Flory–Huggins theory along the lines of Misra et al.[17] (see eq 10b).

Salt Dominance. In the situation where the added salt dominates the screening length the free energy density of mixing of the gel can be defined by a modified excluded-volume parameter, as pointed out by Ross and Pincus.[20] Borue and Erukhimovich[21] have formulated a theory for weakly charged polyelectrolyte solutions. The result of interest here is the modification of the excluded-volume parameter in high salt concentrations. The correction to the excluded-volume parameter is incorporated within the contributions of the translational entropy and electrostatic interactions of the electrolyte ions, since the ion distribution is of the Boltzmann type arising from the PB equation. For the case of salt dominance Borue and Erukhimovich obtain an expression for the effective excluded-volume parameter, which in the present notation translates as:

$$w_{\text{eff}} = w + \frac{\left(\frac{\alpha Z_S}{Z}\right)^2}{2C_b a^3}\left[1 + \frac{2\Phi\alpha Z_S}{C_b Z^2 a^3}\right]^{-1} \tag{8}$$

Here w is the excluded-volume parameter in the absence of electrostatic charges, Z_S is the valence of the polymer segments, and α is their degree of dissociation. The electrolyte concentration (number density) of the symmetric Z:Z electrolyte is C_b. For small charge densities this expression further reduces to

$$w_{\text{eff}} = w + \frac{\left(\frac{\alpha Z_S}{Z}\right)^2}{2C_b a^3} \tag{9}$$

Since the stretching of the chains is balanced by this *effective excluded-volume* parameter, the collapse transition of the gel is dictated by the effective excluded-volume parameter equaling zero. For the present purpose the simple expression of eq 9 will be used to illustrate the swelling and collapse characteristics of mesogels.

Using eq 9 for the effective excluded-volume parameter, one can write the free energy density of mixing of the charged chains in the B domain as follows:

$$F(\Phi) = \frac{w_{\text{eff}}}{2}\Phi^2 = \left[w + \frac{1}{2C_b a^3}\left(\frac{\alpha Z_S}{Z}\right)^2\right]\frac{\Phi^2}{2} \tag{10}$$

The density saturation limit is easily accounted for by a Flory–Huggins expression of the following type:

$$F(\Phi) = (1-\Phi)\ln(1-\Phi) + \chi\Phi(1-\Phi) + \frac{1}{2C_b a^3}\left(\frac{\alpha Z_S}{Z}\right)^2\frac{\Phi^2}{2} \tag{10b}$$

With $w = (1 - 2\chi)$, the above expression reduces to eq 10 as $\Phi \to 0$. In this work we use eq 10, instead of eq 10b, for simplicity.

Another quantity of interest is the potential of mean force acting upon each segment. This is defined as:

$$U(\Phi) = -\frac{\partial}{\partial\Phi}F = -w_{\text{eff}}\Phi \tag{11}$$

The potential of mean force plays a central role in determining the size of the loops, ξ, and the fraction of bridging segments, q, in the central region. This is discussed later in section 3.3.

No Salt. This limit has been explored for polyelectrolyte brushes by Borisov et al.[18] and by Ross and Pincus.[20] In the no salt limit the counterions are strongly confined to the polymer brush. The dominant contribution to the free energy density of mixing from the polyelectrolyte charges arises from the confinement of the counterions to the swollen B domain. As in the cases of Borisov et al. and Ross and Pincus we assume that the counterions are tightly bound to the polymer chains and that the volume fraction accessible to the counterions equals the volume occupied by the polymer. In this case one can write the free energy density of mixing as:

$$F(\Phi) = \frac{w}{2}\Phi^2 + \alpha Z_S\Phi\ln\Phi \tag{12}$$

The corresponding potential of mean force is then

$$U(\Phi) = -\frac{\partial}{\partial \Phi}F = -w\Phi - \alpha Z_S(\ln \Phi + 1) \qquad (13)$$

3.2. Stretching Energy. Bridges span two regions, the bridge and loop region near the interfaces and the central region. The stretch in these two regions is, in general, not equal and depends upon the value of q, the fraction of bridge segments belonging to the central region, and ξ, the size of the loops. The value of q, as shown later, is determined by the constraint that the sum of the stretch and the mean-field potential (the Hamiltonian) is the same for all segments along the chain contour at equilibrium. The stretch contribution of each bridging chain, assuming Gaussian stretch energy, can be written in dimensionless form as:

$$T_B = \frac{N}{2}\beta^2\left[\frac{(1-\xi)^2}{q} + \frac{\xi^2}{1-q}\right] \qquad (14)$$

The first term in the brackets is the contribution of the bridge segments in the central region and the second term is the contribution of the bridge segments in the bridge and loop region, next to the A–B interfaces.

The stretching energy of each loop can be similarly written as:

$$T_L = \frac{N}{2}\beta^2\xi^2 \qquad (15)$$

3.3. Free Energy Profiles. Using the above expressions for the free energy densities of mixing (eqs 10 or 12) and for the stretching energies (eqs 14 and 15), one can write an expression for the free energy profile of the B domain (on a unit interfacial area basis) as follows:

$$G(\beta) = \bar{\sigma}(1-f)T_B + \bar{\sigma}(1-f)T_L + N\beta(1-\xi)F\{\Phi_B\} + N\beta\xi F\{\Phi_{BL}\} \qquad (16)$$

There are, however, two variables that need to be determined before one can compute the above expression. These are the loop size, $\xi(\beta)$, and the fraction of bridge segments in the central zone, $q(\beta)$. One therefore needs two more expressions in order to uniquely define $G(\beta)$ (the free energy profile). One of these arises from the condition that the sum of the stretch and the mean field potential (the "constant of motion") remains unchanged as one travels along the contour of the chain.[22] The other arises from the fact that in an equilibrium situation, for a given domain size β, the loop size will adjust in order to minimize the free energy.

Constant of Motion. A bridge segment in the central region has a mean-field potential that is different from that of a bridge segment in the bridge and loop region, since both regions have different polymer volume fractions. However, in the classical picture, as Shim and Cates[22] point out, the sum of the stretch and the mean-field potential should be constant along the chain contour. In other words

$$\frac{1}{2}\left(\frac{d\mathbf{r}(n)}{dn}\right)^2 + U(n) = H = \text{constant} \qquad (17)$$

Here $\mathbf{r}$ is the coordinate of the nth segment, $U(n)$ is the potential of the nth segment, and H is the "constant of motion". The chains will always rearrange in order to satisfy this equality. Thus the fraction of bridge segments in the central region is fixed by the following mathematical expression:

$$\frac{\beta^2(1-\xi)^2}{2q^2} + U(\Phi_B) = \frac{\beta^2\xi^2}{2(1-q)^2} + U(\Phi_{BL}) \qquad (18)$$

Φ_B and Φ_{BL} depend upon q and ξ through eqs 4 and 5, and therefore eq 18 essentially involves the latter pair as the variables.

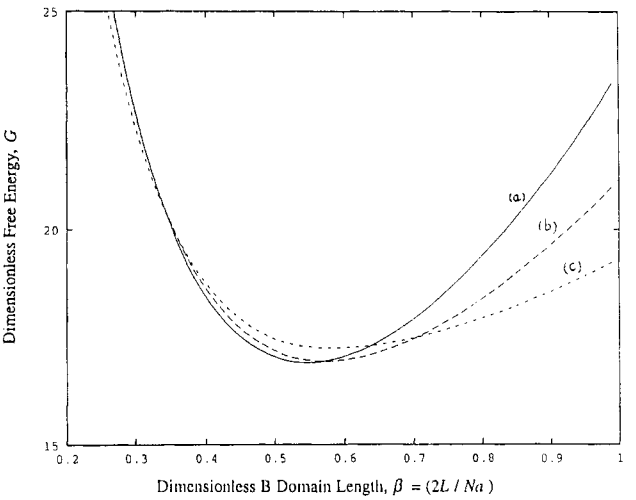

Figure 2. Free energy, $G(\beta)$, profiles for the salt dominance case. The chains, in this figure and in the rest of the figures, contain 1000 segments, and the tethering density is 0.05. The other parameters are, $(\alpha Z_S/Z) = 0.25$, $C_b = 0.001$ M, and $w = -0.5$. The loop fractions are (a) 0.4, (b) 0.6, and (c) 0.8.

Size of the Loops. As the B domain size, β, is varied, the loops rearrange to a size that minimizes the free energy of the system. The fact that loops can relax to minimize the free energy of the structure can be mathematically expressed as:

$$\partial G\{\beta,\xi,q\}/\partial\xi = 0 \qquad (19)$$

Equation 19 also involves q and ξ as variables. We thus have two equations, eqs 18 and 19, involving the unknowns ξ and q which need to be solved simultaneously in order to obtain $G(\beta)$, the free energy profile.

The equilibrium dimensions of the gel are defined by the local minima in the free energy profile subject to the constraint $\beta_{min} < \beta < 1$.

3.4. Pressure Profile. We define a dimensionless force per unit area of the lamellar interface (or pressure), necessary to compress or elongate the swollen mesogels as:

$$P = \partial G/\partial\beta \qquad (20)$$

In this notation a positive value of the pressure, P, implies that the system is in the elongation regime, while a negative pressure implies that the system is compressed.

4. Results and Discussion

All results are presented in the form of nondimensional quantities. In all the cases explored here the B blocks contained (N=) 1000 segments. The tethering density was also held constant at $\bar{\sigma} = 0.05$.

4.1. Salt Dominance. All results discussed in this subsection correspond to the free energy density of mixing as given by eq 10 and the mean-field potential of a segment as given by eq 11.

In Figure 2 three free energy profiles are shown for loop fractions of 0.4, 0.6, and 0.8. The asymmetry between compression and elongation is quite obvious from this figure. As the fraction of loops increases fewer bridging chains are forced to stretch upon elongation and also a larger fraction of chains in the loop conformation can relax to a minimum free energy conformation. Thus a free energy increase upon elongation decreases with increasing number of loops. In compression both loops and bridges get compressed almost equally, and moreover it is the excluded-volume term that is dominant compared to the

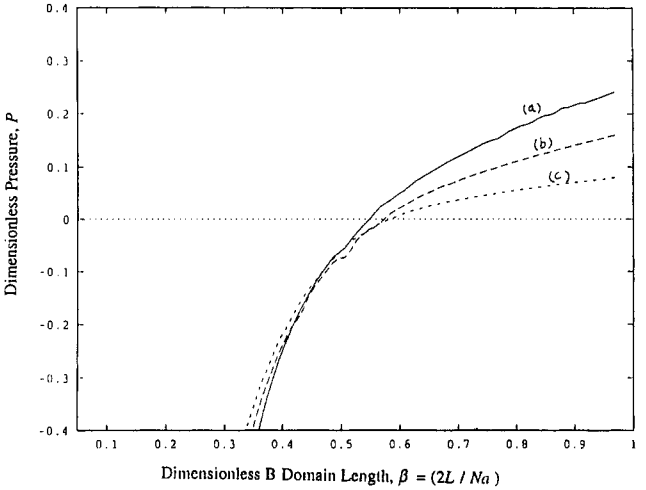

Figure 3. Pressure profiles, $P(\beta)$, corresponding to the free energy profiles of Figure 2 (i.e., salt dominance case). The loop fractions are (a) 0.4, (b) 0.6, and (c) 0.8.

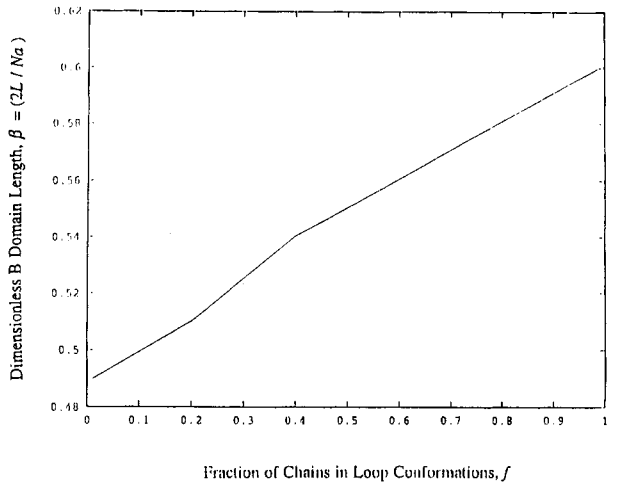

Figure 4. Size of the B domain as a function of the loop fraction in the salt dominance case. The parameters are $\alpha Z_S/Z = 0.25$, $C_b = 0.001$ M, and $w = -0.5$.

stretch energy. Thus the free energy profiles converge upon compression.

Pressure profiles corresponding to the above free energy profiles are shown in Figure 3. The pressure profiles diverge upon elongation, indicating that the stretching of the gel strongly depends upon the fraction of loops. Indeed the force needed to elongate the gel drops with increasing loop fraction since fewer bridges are forced to stretch. The situation for compression, however, is quite the opposite. Here the compression force is nearly independent of the fraction of loops in the system. The x intercepts mark the points of zero force and therefore correspond to the equilibrium dimensions of the mesogel. Note that the intercepts, and the equilibrium dimensions, change with the loop fraction.

The equilibrium dimensions of a mesogel, like those of a brush, are determined by a balance between stretching and excluded-volume and electrostatic forces. The fewer the bridges, the more they need to stretch before the swelling due to the excluded volume and electrostatics is overcome. Thus increasing the number of loops leads to an increase in the equilibrium dimensions of the mesogel. This is depicted in Figure 4 where the equilibrium B domain size is shown as a function of the fraction of loops. The increase in dimensions of the mesogel is quite substantial with increasing the loop fractions.

The equilibrium dimensions of the B domain are shown as a function of the excluded-volume parameter in Figure

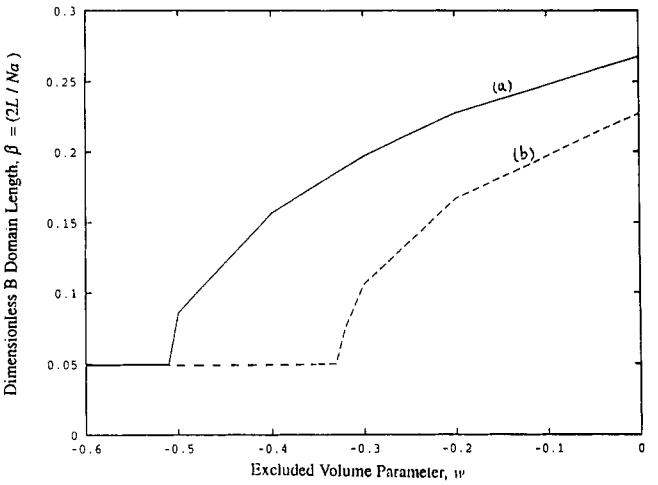

Figure 5. Size of the B domain as a function of the excluded-volume parameter, w, in the salt dominance case. The parameters are $C_b = 0.01$ M and $f = 0.5$. The charge fractions are (a) 0.25 and (b) 0.2.

5. One can also consider the change in the excluded-volume parameter as a change in the temperature. For a B block showing an upper critical solution temperature (UCST) one could look at the excluded-volume parameter as:[23]

$$w = w_0\left(1 - \frac{\theta}{T}\right) \tag{21}$$

where T is the temperature and θ is the theta temperature. For highly negative excluded-volume parameters the electrostatic forces are not strong enough to solvate the B block. As the excluded-volume parameter increases one reaches a point where the effective excluded-volume parameter, as given by eq 9, equals zero. At this point one has a continuous transition from the collapsed to the swollen state. With further increase in the excluded-volume parameter (or temperature) the *effective* excluded-volume parameter becomes positive and the gel swells. These results are very much in line with the results of Halperin for polymer brushes in poor solvents, in that the transition from the collapsed to the swollen state is continuous.[24]

According to eq 9, increasing electrostatic repulsions, characterized by an increase in the backbone charge density or a decrease in the electrolyte concentration, increase the effective excluded-volume parameter. This means that with increasing the strength of electrostatics the collapse transition gets depressed to a lower value of the excluded-volume parameter (or lower temperature for a polymer with UCST). This can be seen in Figure 5 where the curve for the larger backbone charge density shifts the transition to a lower excluded-volume parameter (or lower temperature).

4.2. No Salt. All the results in this subsection correspond to the free energy density of mixing as given by eq 12 and the mean-field potential of the segments given by eq 13.

We look again at the free energy profiles for various loop fractions in Figure 6. For the no salt case the picture is more interesting. As one focuses on the free energy profile for a loop fraction of 0.4, one notices two minima in the free energy profile, separated by a substantial energy barrier. Thus one can have two states, one the *metastable* collapsed minimum at $\beta_{min} = \bar{\sigma}$ and the stable minimum at an extended state of $\beta_{equil} \sim 0.35$. This result is similar to the result obtained by Ross and Pincus for polyelectrolyte brushes. However, for a mesogel, the additional factor of the loop fraction can bring into existence a metastable collapsed minimum. The lifetime of

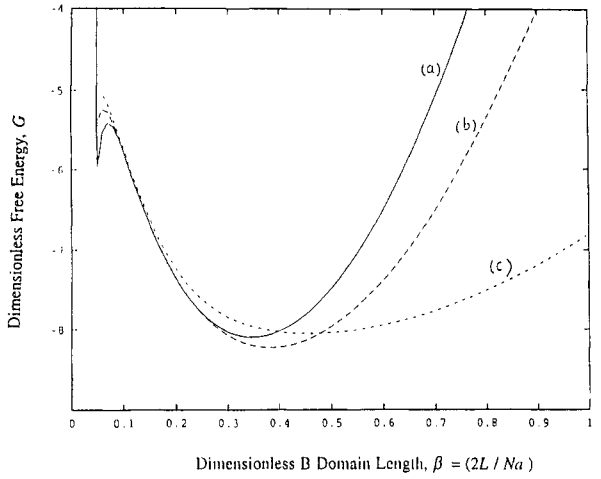

Figure 6. Free energy, $G(\beta)$, profiles for the no salt case. The parameters are $\alpha Z_S = 0.1$ and $w = -0.2$. The loop fractions are (a) 0.4, (b) 0.6, and (c) 0.9.

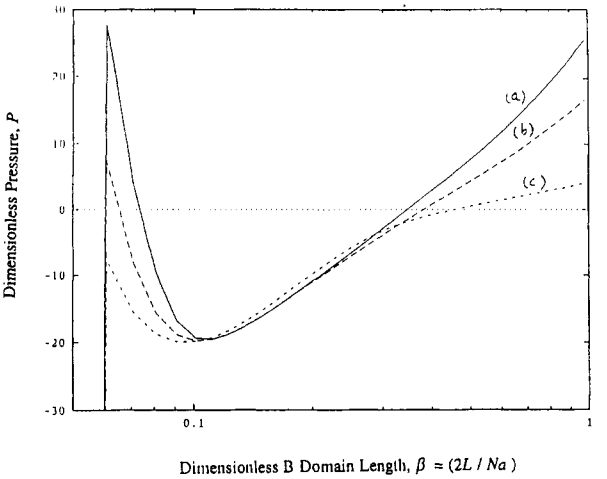

Figure 7. Pressure profiles, $P(\beta)$, corresponding to the free energy profiles in Figure 6. The loop fractions are (a) 0.4, (b) 0.6, and (c) 0.9.

this collapsed state would depend upon the energy barrier and on polymer dynamics—a discussion of this aspect is outside the scope of this manuscript. The profile for a loop fraction of 0.6 also shows two minima, but the minimum at the collapsed state is less pronounced now—presumably the lifetime of the state is shorter. Indeed this is the result of a smaller "attractive" stretching force due to the decrease in the number of bridges. On further increasing the loop fraction to 0.9, one finds that the collapsed minimum has disappeared completely and that only one equilibrium state remains. Indeed there is a transition at a critical loop fraction (in this case 0.83) where the collapsed minimum becomes metastable. The other qualitative features of loop fraction dependence remain, viz., the asymmetry of stretching and compression. However, close to the collapsed minimum, the compression is strongly dependent upon the loop fraction for the no salt case in the contrast to the salt dominance case.

The loop fraction at which the collapsed minimum becomes metastable can be characterized as follows. Note that as the loop fraction increases the slope of the free energy curve (or the pressure) at the collapsed minimum ($\beta = \beta_{min} = \bar{\sigma}$) decreases and must equal zero at the critical loop fraction. In other words, the critical loop fraction, f^*, would satisfy the following equality (for a given charge fraction and excluded-volume parameter):

$$\left[\frac{\partial G}{\partial \beta}\right]_{\beta=\bar{\sigma},f=f^*} = 0, \quad \text{const}(\alpha Z_S, w) \tag{22}$$

For $f < f^*$ the mesogel will have two possible states; for $f > f^*$ there will be only one extended equilibrium state. While an analytical expression for f^* is not easily evaluated, a simple numerical procedure would yield the phase diagram for the system of interest (as shown later in Figure 8).

In Figure 7 are shown the pressure profiles corresponding to the energy profiles above. The pressure profile has more features now compared to the salt dominance case. There are three intercepts, in general, of the pressure profile with the x axis. The largest intercept, of course, corresponds with the extended state. The middle intercept corresponds with the energy barrier, and the final intercept marks the collapsed minimum. Note that these last two intercepts vanish above the critical loop fraction of 0.83, marking the existence of only one possible state.

The transition from two possible states (one stable and one metastable) to a single extended state is depicted in Figure 8. Here the B domain size is shown as a function of the loop fraction. Below the loop fraction of 0.83 both

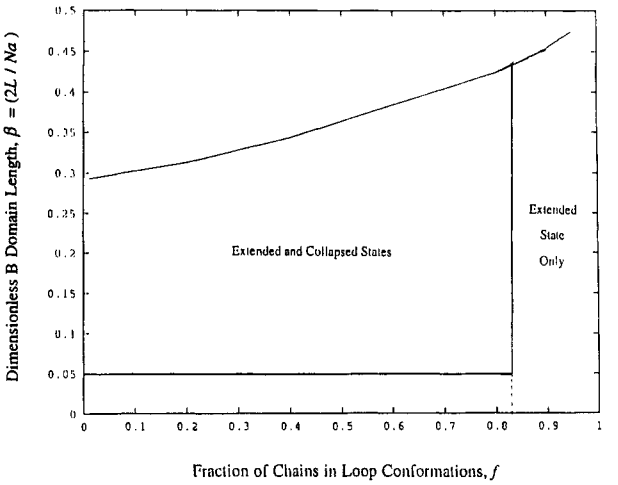

Figure 8. Size of the B domain as a function of the loop fraction. The parameters are $\alpha Z_S = 0.1$ and $w = -0.2$. The vertical line at $f = 0.83$ delimits the region of two states from that of only one extended state.

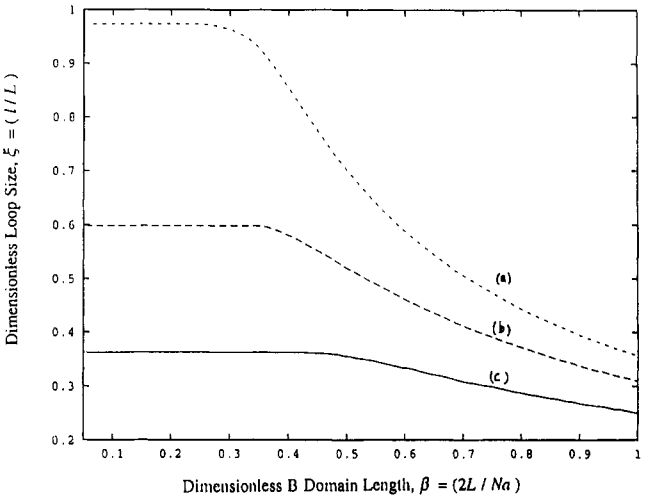

Figure 9. Size of the loops, ξ, as a function of the B domain size, β, for various loop fractions in the no salt case. The parameters are $\alpha Z_S = 0.1$ and $w = -0.2$. The loop fractions are (a) 0.9, (b) 0.8, and (c) 0.4.

the metastable collapsed and the stable extended states are possible, while above that loop fraction only the extended state can exist.

The reason for this is apparent from Figure 9. Here we have shown the fractional loop size, ξ, as a function of the β domain size for different loop fractions. Notice that the

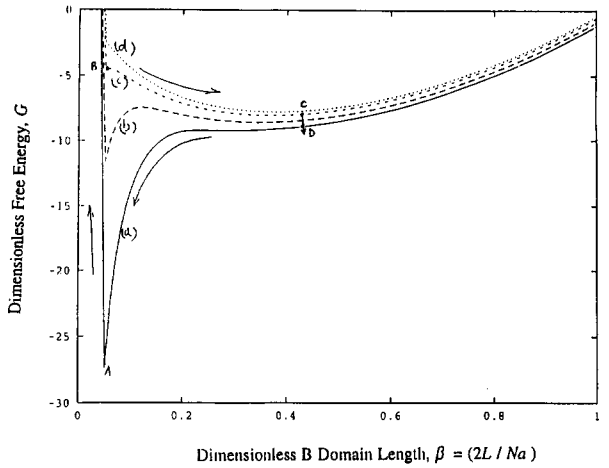

Figure 10. Free energy profiles, $G(\beta)$, for different values of the excluded-volume parameter, in the no salt case. The parameters are $\alpha Z_S = 0.1$ and $f = 0.5$. The excluded-volume parameters are (a) −0.42, (b), −0.3, (c) −0.17, and (d) −0.1.

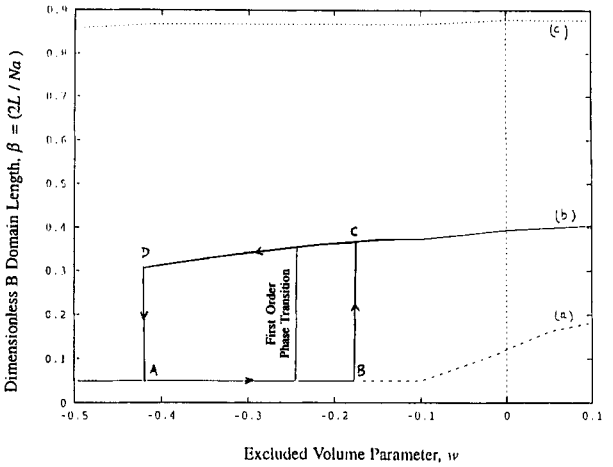

Figure 11. Size of the B domain as a function of the excluded-volume parameter, w, in the no salt case. The loop fraction is $f = 0.5$. The charge fractions αZ_S are (a) 0.01 and (b) 0.1 (a first-order phase transition between the extended and collapsed states occurs at $w = -0.25$) and (c) 0.5.

limiting loop size remains less than unity until the loop fraction approaches unity. If the loop fraction is unity, the situation corresponds to two opposing brushes composed of loops and the interaction is purely repulsive. One can now replace some of the loops with bridges. If the loop size, ξ, remained unity, then the situation is essentially unchanged energetically since the loops and bridges are completely equivalent. However, as seen in Figure 9, once some bridges are formed, the remaining loops can relax to a smaller size, creating two regions of differing segment densities. The bridges then provide a net attractive force between the interfaces. This is what leads to the behavior observed in Figures 6–8.

In Figure 10 are shown four free energy profiles for four different values of excluded-volume parameters (or temperatures). Features similar to Figure 6 are immediately obvious. There are, in general, two possible states, at the collapsed minimum and at an extended state around $\beta \sim 0.4$. The other pertinent features are the relative magnitudes of the two minima and the energy barrier between them. Curve (a) corresponds to a critical excluded-volume parameter (or temperature) where the extended minimum disappears and the system falls into the collapsed minimum which is the only stable state. As one increases the excluded-volume parameter (or temperature), the collapsed minimum becomes smaller in magnitude and a metastable extended state, separated by an energy barrier, comes into existence. At some stage the two states have the same energy and are both stable—the transition between the two is of the first order. On a further increase of the excluded-volume parameter the collapsed minimum becomes metastable and ultimately disappears and the extended state is the only equilibrium state. Curve (c) corresponds to the critical excluded-volume parameter where the collapsed minimum just disappears. The transitions between the extended and the collapsed states are discontinuous, unlike the salt dominance case. The conditions for these transitions have recently been established by Ross and Pincus[20] for an Alexander–de Gennes brush which corresponds to the case of all bridges ($f = 0$). The transitions for the mesogel will also follow these general conditions except that the critical parameters will be modified to include the effect of the loop fraction. It is easy to see that as the fraction of loops increases the attractive bridging force decreases. Thus the excluded-volume parameters would have to be more negative and the charge fraction lower, compared to the Ross and Pincus brush,[20] before the mesogel collapses.

Another interesting phenomenon is the appearance of hysteresis. If one starts at point A (Figure 10) and increases the excluded-volume parameter (following the arrow), say, by increasing the temperature, the gel remains collapsed until one reaches point B (corresponding to the critical excluded-volume parameter where the collapsed state disappears). Here the system "slides" into the extended minimum at point C. Now, however, a decrease in the excluded-volume parameter (or temperature) traps the system in the extended minimum until point D is reached (which corresponds to the critical excluded-volume parameter where the extended minimum disappears). The system now slides back to the collapsed minimum at point A. Again, these points on the hysteresis curve mark the region where the states just become metastable. Practically hysteresis would be observed between states that have appreciable lifetimes, i.e., when the energy barrier separating the metastable state from the stable state is high enough—the observed behavior would therefore be dependent upon polymer dynamics. Thus one would expect the two excluded-volume parameters where hysteresis would be observable to lie between those depicted in the figure.

Thus a polyelectrolyte mesogel will exhibit hysteresis in the absence of salt, quite like the case of polyelectrolyte brushes discussed by Ross and Pincus (but with modified critical transitions). By contrast the salt dominance case exhibits no hysteresis.

Figure 11 depicts the equilibrium dimensions of a mesogel, in the absence of mobile electrolyte, as a function of the excluded-volume parameter. For very low values of backbone charge densities the crossover between the collapsed and extended states is continuous as in the case of salt dominance. This is the case for curve (a). Upon increasing the backbone charge, as shown by Ross and Pincus, a critical charge fraction is reached where the two states, extended and collapsed, come into existence (at least for some range of the excluded-volume parameter). When these states are of equal energy, a first-order phase transition occurs between the two. This corresponds to the excluded-volume parameter of −0.25. The hysteresis path corresponding to Figure 10 is also traced out on curve (b). States with appreciable lifetimes would probably be obtained somewhere between the two ends where one or the other state becomes metastable (i.e., between $w = -0.17$ and $w = -0.42$). One qualitative feature corresponding to the salt dominance case can still be seen. This is the

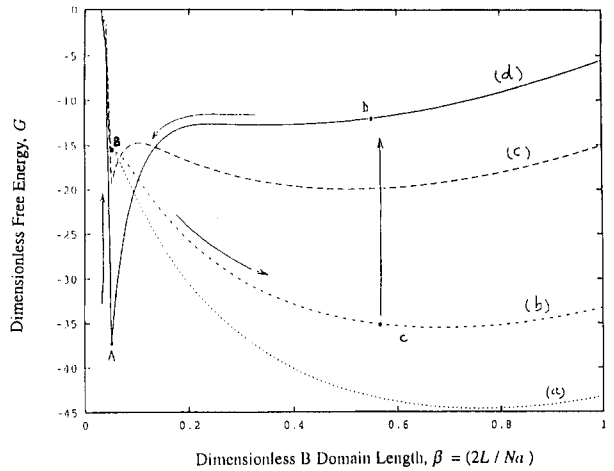

Figure 12. Free energy profiles, $G(\beta)$, for different values of the charge fraction, in the no salt case. The parameters are $w = -0.6$ and $f = 0.5$. The charge fractions αZ_S are (a) 0.4, (b) 0.33, (c) 0.2, and (d) 0.13. A first-order phase transition between the extended and collapsed states occurs at $\alpha Z_S = 0.29$.

depression of the critical excluded-volume parameter with an increase in the backbone charge density.

A similar hysteresis can be observed for the change in backbone charge density (which, at least for weak polyelectrolytes, can be varied by changes in the pH of the solution). In Figure 12 are shown four free energy profiles corresponding to four different values of backbone charge (or pH). It is obvious that for low backbone charges the collapsed minimum is quite pronounced and that there in no extended state. As the backbone charge density increases, an extended minimum appears which is separated from the collapsed minimum by an energy barrier. With increasing backbone charge the collapsed minimum becomes smaller until the energies of the collapsed and extended minima are equal and a first-order phase transition between the two occurs. A further increase in charge leads to the disappearance of the collapsed minimum. The appearance of metastable collapsed and extended minima is again characterized by critical backbone charge densities (or pH) (the lower and upper bounds in this case are $\alpha Z_S = 0.13$ and $\alpha Z_S = 0.33$, respectively). The first-order transition takes place at $\alpha Z_S = 0.29$. The hysteresis path for this case is marked on the free energy diagram, as we go from point A to D and back to A. The variation of equilibrium dimensions with backbone charge (or pH) will appear similar to that for equilibrium dimension versus the excluded-volume parameter in Figure 11.

5. Conclusions

A mean-field theory for swollen *polyelectrolyte* mesogels is developed in this study. Of interest here were the free energy and pressure profiles of swollen mesogels as affected by the loop (or bridge) fraction as well as the relative strengths of the electrostatic and excluded-volume forces. The effects of electrostatics were explored at both limits—high mobile electrolyte concentration (or salt dominance) limit and the no electrolyte limit.

The high salt concentration limit, treated along the lines of Borue and Erukhimovich,[21] is characterized by an effective excluded-volume parameter approach that amounts to adding a correction term to the excluded-volume parameter of the uncharged chain, as shown in eq 9. In the salt dominance regime the transition from collapsed to swollen state is continuous and characterized by the effective excluded-volume parameter equaling zero—in agreement with transitions in polymer brushes.[24] The critical excluded-volume parameter is depressed to lower values as the electrostatic forces grow stronger. The critical transition charge densities or the critical excluded-volume parameters are independent of the loop or bridge fraction in this limit. The effect of the increasing loop fraction is reflected in the increasing asymmetry of compression and elongation. The loop fraction significantly affects the free energy and pressure profiles in the elongational regime, while these profiles converge in the compression regime. The equilibrium dimension of the mesogel is seen to increase with an increase in the fraction of loops, owing to loss of the bridging "attraction" between the opposing lamella.

The no salt limit, treated along the lines of Ross and Pincus,[20] shows interesting features. The collapse transition for moderate values of charges or moderately negative excluded-volume parameters is now discontinuous, very much in agreement with the result of Ross and Pincus for polyelectrolyte brushes. However, in the case of mesogels these transitions are also affected by the loop fraction. The Ross and Pincus brush corresponds to the special case of no loops.[25] As the loop fraction increases, the strength of the collapsed free energy minimum decreases until at a critical loop fraction the collapsed state disappears completely. The critical values of charge and excluded-volume parameters of the Ross and Pincus brush present the upper bounds for the mesogel—the depression of these points depending upon the loop fraction. The presence of two possible states for the no salt limit leads to interesting hysteresis behavior also. The transitions for low charge densities and slightly negative excluded-volume parameters, as for the Ross and Pincus brush, are continuous.

References and Notes

(1) de Gennes, P.-G. *Scaling Concepts in Polymer Physics*; Cornell University Press: Ithaca, NY, 1979.
(2) Bates, F.; Fredrickson, G. H. *Annu. Rev. Phys. Chem.* **1990**, *41*, 525.
(3) Halperin, A.; Tirrell, M.; Lodge, T. P. *Adv. Polym. Sci.* **1992**, *100*, 31.
(4) Halperin, A.; Zhulina, E. B. *Europhys. Lett.* **1991**, *16*, 337.
(5) Halperin, A.; Zhulina, E. B. *Macromolecules* **1992**, *25*, 5730.
(6) Rabin, Y.; Alexander, S. *Europhys. Lett.* **1990**, *13*, 49.
(7) Halperin, A.; Zhulina, A. B. *Macromolecules* **1991**, *24*, 5393.
(8) Goodman, I., Ed. *Developments in Block Copolymers—2*; Applied Science: New York, 1985.
(9) Feast, W. J., Munro, H. S., Eds. *Polymer Surfaces and Interfaces*; Wiley: New York, 1987.
(10) Patel, S.; Tirrell, M.; Hadziioannou, G. *Colloids Surf.* **1988**, *31*, 157.
(11) Alexander, S. *J. Phys. (Paris)* **1977**, *38*, 983.
(12) de Gennes, P.-G. *Adv. Colloid Interface Sci.* **1987**, *27*, 189.
(13) Semenov, A. N. *Sov. Phys. JETP* **1985**, *61*, 733.
(14) Milner, S. T.; Witten, T. A.; Cates, M. E. *Macromolecules* **1988**, *21*, 2610.
(15) Johner, A.; Joanny, J. F. *Europhys. Lett.* **1991**, *15*, 265.
(16) Miklavic, S. J.; Marcelja, S. *J. Phys. Chem.* **1988**, *92*, 6718.
(17) Misra, S.; Varanasi, S.; Varanasi, P. P. *Macromolecules* **1989**, *22*, 4173.
(18) Borisov, O. V.; Birshtein, T. M.; Zhulina, E. B. *J. Phys. II* **1991**, *1*, 521.
(19) Pincus, P. *Macromolecules* **1991**, *24*, 2912.
(20) Ross, R.; Pincus, P. *Macromolecules* **1992**, *25*, 2177.
(21) Borue, V. Yu.; Erukhimovich, I. Ya. *Macromolecules* **1988**, *21*, 3240.
(22) Shim, D. F. K.; Cates, M. E. *J. Phys. Fr.* **1989**, *50*, 3535.
(23) Flory, P. J. *Principles of Polymer Chemistry*; Cornell University Press: Ithaca, NY, 1971.
(24) Halperin, A. *J. Phys. Fr.* **1988**, *49*, 547.
(25) Ross and Pincus have recently discussed (*Europhys. Lett.* **1992**, *19*, 79) the possible existence of another state for uncharged "twice grafted" brushes, corresponding to the case of no loops ($f = 0$). They show that the collapse may be preempted by lateral segregation of chains, i.e., density fluctuations in the lateral directions. Though it is beyond the scope of a mean field theory, this phase behavior would be of direct interest to the swelling/collapse of mesogels as well.